Int J Clin Exp Pathol (2008) 1, 169-179
www.ijcep.com/IJCEP708001

Original Article

Yellow Fever Virus Infection in Syrian Golden Hamsters: Relationship between Cytokine Expression and Pathologic Changes

Guangyu Li[1], Tao Duan[1], Xiaoyan Wu[1, 3], Robert B. Tesh[1], Lynn Soong[1, 2] and Shu-Yuan Xiao[1]

[1]Department of Pathology and Center for Biodefense and Emerging Infectious Diseases, Institute for Human Infections and Immunity; [2]Department of Microbiology and Immunology, University of Texas Medical Branch, Galveston, TX 77555, USA; [3]Department of Medicine, Zhong Nan Hospital, Wuhan University, Wuhan, Hubei Province, China

Received 1 Aug 2007; accepted and available online 26 Aug 2007

Abstract: Infection of primates by yellow fever virus (YFV) often results in severe multi-organ failure with marked histologic abnormalities. However, the role of host's immune response, particularly innate immunity, in disease process is unclear. In this study, we used a well established hamster model of yellow fever to examine the dynamic changes of cytokine expression and histopathology in the liver, spleen, kidney, and heart during the course of YFV infection. We observed that the levels of inflammatory cytokines (IFN-γ, IL-2, TNF-α) in the liver were significantly reduced in the mid-stage of infection (8 days), but were elevated later (12 days). In contrast, IL-12p40 was elevated throughout the infection. The levels of IFN-γ, IL-2, and TNF-α were increased in the spleen, kidney, and heart throughout the study period. For regulatory cytokines, IL-10 was significantly increased, and TGF-β was reduced in the liver, spleen and heart in both early and mid-stages of infection, but was elevated in the kidney during the entire course of infection. In view of the pathologic changes, the observed cytokine profiles suggest that YFV has immunosuppressive effects, which contribute to liver damage in the mid-stage of infection, followed by an immunopathogenic mechanism that leads to disease progression during the late-stages of infection. Our findings support the hypothesis that organ injury by YFV is probably due to a combination of multiple factors, including direct viral injury and host innate immune responses.
Key Words: Yellow fever virus, pathogenesis, cytokines, RT-PCR, pathology, immunohistochemistry

Introduction

Yellow fever virus (YFV), a mosquito-borne flavivirus (family *Flaviviridae*), can cause severe systemic illness in humans, characterized by fever, hepatic failure, renal and myocardial injury, hemorrhage, with high mortality [1-4]. Although a highly effective vaccine is available, it is underutilized, and consequently, yellow fever (YF) remains an important cause of morbidity and mortality in tropical regions of sub-Saharan Africa and South America [5]. The potential for its re-emergence into urban areas in the future still exists. Because of the sudden onset and rapid progression of the disease in humans, only limited knowledge is available regarding the pathogenesis and immune response during YFV infection. Most of the pathologic descriptions in patients died of YF are based on studies of autopsies. Abnormalities have been described in the liver, spleen, kidneys, heart and lymph nodes; however, these changes were observed during the terminal stage of YF [6-9]. A spectrum of histologic changes has been observed in Syrian golden hamsters experimentally infected with the YFV [10, 11]. Among the multiple organs involved, the changes in the liver and spleen are the most striking [11]. The splenic pathology is characterized by the presence of large lymphocytes, plasma cells, and histiocytes, and the disappearance of small lymphocytes. Although the severity of the histopathologic changes in the liver, spleen, kidneys, and heart correlate with the clinical symptoms observed in patients, the basic patho-physiologic process involved is largely

unknown. For example, it remains unclear the relative contributions of direct cytopathic effect of YFV and host immune responses in tissue damage. Previous studies have shown that cytotoxic T lymphocytes (CTL) mediate killing of flavivirus-infected cells and contribute to viral clearance during primary YFV infection. $CD4^+$T helper cells are critical for protection of mice from YFV infection [12]; these cells also secrete inflammatory cytokines that can result in cell death [13, 14].

The current study was intended to address these questions by investigating the potential roles of innate immunity, particularly cytokine expression, in YFV infection. In addition, the relationships between the cytokine expression profiles and histopathologic changes in individual organs were examined.

Materials and Methods

Animals

Female Syrian golden hamsters (*Meso-cricetus auratus*, Harlan Sprague Dawley Indianapolis, IN), 9-10 week old, were used in the experiment. Animals were housed in a BSL-3 animal facility under protocols approved by our Institutional Animal Care and Use Committee (IACUC).

Virus

The Jimenez strain of YFV was used in this study. This virus was originally isolated from a fatal human case in Panama in 1974. It had subsequently subjected to 10 serial passages in adult hamsters to increase the virulence [10]. The titer of the virus stock was $10^{7.7}$ tissue culture infectious $dose_{50}$ units/mL ($TCID_{50}$/mL).

Infection of Hamsters and Tissue Collection

Four hamsters were used as uninfected controls. Twenty-four additional hamsters were each inoculated intraperitoneally with 0.1 mL of the virus stock. On days 1, 3, 6, 8, 12 and 16 post-infection (p.i.), 4 hamsters were anesthetized with Halothane and blood was collected for viral titration and liver function assays. The animals were then exsanguinated by cardiac puncture and immediately necropsied. Samples of liver, spleen, kidney and heart were collected and divided into two parts. One part was placed in 10% formalin for histopathologic examination; the other was put into Trizol (Invitrogen, Carlsbad, CA) for RNA extraction.

Histologic Preparation and Evaluation

After fixation in 10% formalin for 24 h, the tissues were transferred to 70% ethanol. Subsequently, the fixed tissues were processed in an automatic tissue processor (Tissue-Tek VIP E300; Sakura) and embedded in paraffin. Routine hematoxylin & eosin (H&E) stained slides were prepared, and examined microscopically as described previously [11]. Additional unstained slides were prepared for subsequent immunohistochemical (IHC) studies (see below).

Immunohistochemical Detection of YFV Antigen

After deparaffinization, tissue sections were immersed in 3% H_2O_2 for 20 min, and followed by antigen retrieval using 10% target-retrieval solution (DAKO, Carpinteria, CA) at 90°C for 30 min. YFV-specific mouse immune ascetic fluid was diluted 1:100 and applied to the sections overnight at 4°C. To eliminate cross-species nonspecific reactions, an ISO-IHC AEC kit (InnoGenex, San Ramon, CA) was used to detect YFV antigens.

Virus Titrations

Blood samples were titrated in 24-well culture plates, using C6/36 mosquito cells, as previously described [10, 15]. YFV titers were calculated as the $TCID_{50}$/mL, using the method of Reed and Muench [16].

Liver Function Assay

The levels of total billirubin (TB), serum alanine aminotransferase (ALT), and aspartate aminotransferase (AST) were measured using commercial kits (Sigma Diagnostics, St. Louis, MO).

RNA Extraction and cDNA Preparation

Tissues (100 mg) were put into 0.75 mL of Trizol and homogenized using a pestle. After incubation at room temperature for 5 min, the homogenized samples were subjected to RNA extraction using chloroform and isopropyl alcohol. The RNA pellet was dissolved in 30 μl of RNase-free water and treated with DNA-free

DNase (Ambion, Austin, TX).

For first-strand cDNA synthesis, the Super-Script™ II First-Strand Synthesis System (Invitrogen) was used. Using the random primer in a total reaction volume of 20 µl, each reaction contained 50 units of the SuperScript II RT and 1µg of RNA. Reverse transcription was performed for 10 min at 25°C, followed by 50 min at 50°C, and terminated at 85°C for 5 min. RNase H (1 µl) was added to the reaction and incubated for 20 min at 37°C.

Cytokines and YFV Quantification

Gene expression was analyzed by real-time quantitative RT-PCR. For amplification of cDNA, a forward and reverse primer pair and a specific probe were designed for each cytokine gene. The probe was labeled with reporter dye FAM (6-carboxyfluorescein) at the 5' residue and a black hole quencher (BHQ1) at the 3'-guanidine residue. The primer-probe sets (**Table 1**) were created for hamster interleukin (IL)-2, IL-4, IL-10, IL-12p40, IFN-γ, TNF-α, TGF-ß , and ß-actin, utilizing the program Primer Express (Applied Biosystems, Foster City, CA). Real-time RT-PCR was performed with the Smart Cycler (Cepheid, Sunnyvale, CA). cDNA (1 µl) was added in the TaqMan Universal PCR Master Mix (Applied Biosystems) that included 25 pmol of the FAM-labeled probe, 100 pmol of each primer for a total volume of 20 µl per reaction. Cycling conditions were 2 min at 50°C, 10 min at 95°C followed by 15 sec at 95°C, and 1 min at 60°C for a total of 50 cycles. Each sample was run in duplicate wells. The comparative method was used to analyze the quantification of RNA. Cycle threshold (C_t) values were normalized to ß-actin, as ΔC_t, which was determined by the formula, $\Delta C_t = C_{t\ (target\ gene)} - C_{t\ (ß\text{-}actin\ gene)}$. Fold change was determined by $2^{-\Delta\Delta Ct}$, where $\Delta\Delta C_t = \Delta C_{t\ (infected)} - \Delta C_{t\ (uninfected)}$ [17]. Samples which did not generate a C_t value were given a default value of 50 [18].

For tissue quantification of YF viral load, RNA extracted from the tissues (100 mg) was dissolved in 30 µl of RNase-free water and treated with DNA-free DNase. Real-time RT-PCR was performed with the Smart Cycler. RNA (100 ng) was added in the TaqMan one-step RT-PCR master mix (Applied Biosystems, Branchburg, NJ) that included 50 pmol of the FAM-labeled probe, 200 pmol of each primer for a total volume of 20 µl per reaction. Cycling conditions were 30 min at 48°C for RT, 10 min at 95°C for AmpliTaq Gold DNA polymerase activation, followed by 15 sec at 95°C, and 1 min at 60°C for a total of 50 cycles. Each sample was run in duplicate wells. External standard curves were generated by serial dilutions of RNA, derived from aliquot with known input virus titers, covering a range from 1 $TCID_{50}$ to 1×10^7 $TCID_{50}$. Eight points for standard curve were run in duplicate along with non-template controls to set the threshold value. 5 µl RNA of each sample was used to perform real-time RT-PCR using the one-step PT-PCR master mix as the conditions above. Cycle threshold (Ct) values from each RNA sample were compared with external standard curves to determine related virus loads in each tissue.

Statistical Analysis

Results were expressed as mean ± standard derivation (SD). Statistical differences in cytokine mRNA levels between groups were evaluated by one-way analysis of variance (ANOVA). All data were analyzed with statview software, and $p<0.05$ was considered statistically significant.

Table 1 Primers and probes for real-time RT-PCR analyses of cytokines and YFV quantification in hamster tissues

Cytokine	RT/Reverse primer (genome-sense)	Forward primer(mRNA-sense)	TaqMan probe (mRNA-sense)
INF-γ	CCGGAATCTTGGTGAGCTTCA	CCGGAATCTTGGTGAGCTTCA	TCCATGCTGCTGTTGAAG
IL-10	AGCTGGACAACATACTACTCACTGA	GGTTTGGCAACCCAAGTAACC	CCTTACTGCAGGACTTTAA
TNF-α	CCGATCACCCCGAAGTTCAG	CCTCTTCTCCTTCCTGCTTGTG	CAGGCAGAAGAGGATTG
IL-12p40	CGGGAATCAGAGGAGCTACTG	TGACTGCAATCAGCACTGACTT	TCTTGACGTTGAACTTC
TGF-β	CGGAGACGCCGAAGCA	GACACACAGTACAGTAAGGTCCTT	CTACAACCAACACAACCC
IL-2	CATCTTCCAAGTGAAAGCTTTTGCT	CCAGTGCCTGGAAGAAGAACTT	TCCAGCACGCTCTGCAG
IL-4	CCAGACGCCCTTTCAGCAA	CTGGGAAGCCCTGCAGAT	CACGGAGAAAGACCTC
β-actin	GGTGTGGTGCCAGATCTTCTC	CCCATTGAACACGGCATTGTC	ACCAACTGGGACGATATG
YFV_{NS3}	GAGCGACAGCCCCGATTTCT	AGGTCCAGTTGATCGCGGC	CAACGTCCAGACAAAAC

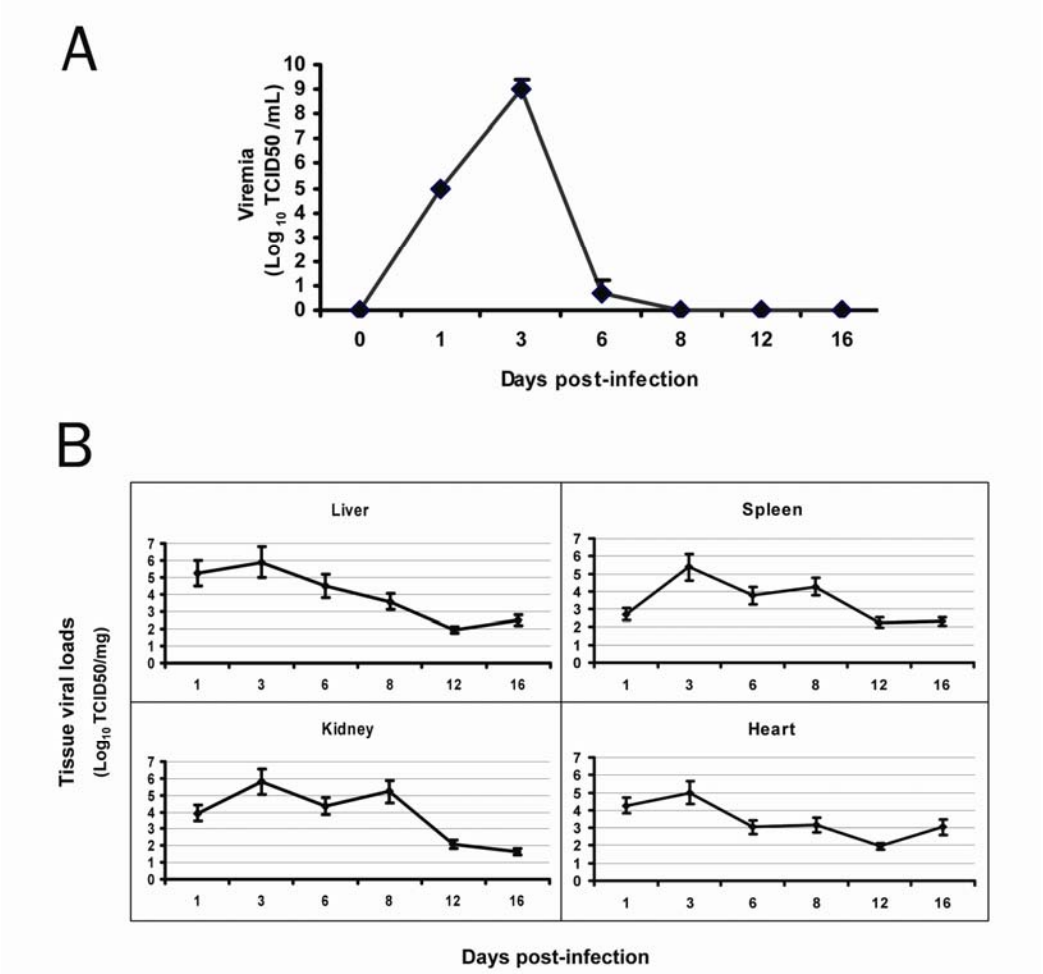

Figure 1 Viremia and YFV tissue load. **A**. Hamsters (4 per group) were infected i.p. with YFV. Serum samples were collected at indicated time points for detecting viremia. Shown are mean ± SD for each group. **B**. Tissue viral loads were detected via one-step PT-PCR using RNA extracted from indicated tissues.

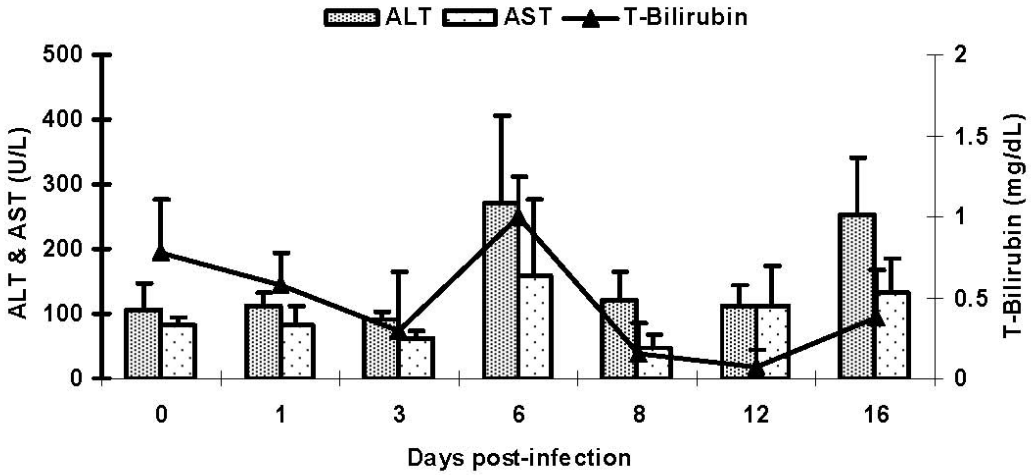

Figure 2 Selected serum chemistry tests of liver damage. Hamsters (4 per group) were infected i.p. with YFV. At indicated time points, liver functions were determined via specific assays. Shown are mean ± SD for each group. T-Bilirubin, total bilirubin; ALT, alanine aminotransferase; AST, aspartate aminotransferase.

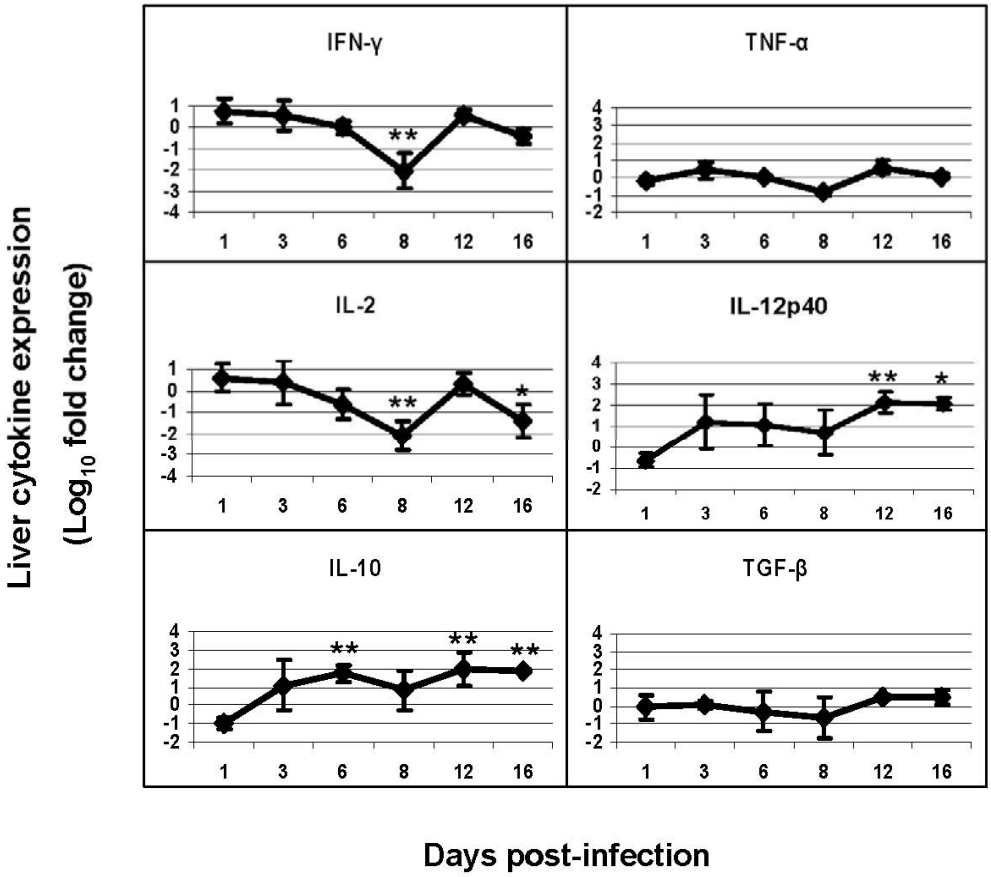

Figure 3 Expression of inflammatory and regulatory cytokines in the livers of YFV-infected hamsters. Mean log_{10} fold change (± SD) are shown for 4 animals per data point. Fold changes vs. control were determined by $2^{-\Delta\Delta Ct}$, where $\Delta\Delta C_t = \Delta C_{t\ (infected)} - \Delta C_{t\ (uninfected)}$ and $\Delta C_t = C_{t\ (target\ gene)} - C_{t\ (ß\text{-}actin\ gene)}$. * and ** indicate $p<0.05$ and $p<0.01$, respectively, between infected and uninfected animals.

Results

Viremia and YFV Loads in Tissues

The pattern of viremia in the infected hamsters (n= 4/day) is summarized in **Figure 1A**. The hamsters developed detectable viremia in one day after infection, which lasted for 5 or 6 days. Peak blood virus titers occurred on day 3 after infection. Tissue viral loads as detected by RT-PCR showed similar patterns but lasted longer (**Figure 1B**).

Pathology and Cytokine Responses in the Liver

The ranges for TB, AST, and ALT in normal adult golden hamsters are 0.4-0.8 mg/dL, 65.3-83.9 U/L, and, 79.5-110.5 U/L, respectively [19, 20]. On the basis of these reference values, the AST level in the infected hamsters was increased on day 6, and was decreased on day 8 (**Figure 2**). The serum mean ALT level, a more specific measurement of hepatic necrosis, was markedly elevated on days 6 and 16. TB also increased significantly on day 6, but went back to normal level on day 8, and was elevated again on day 16.

Microscopically, by day 3, mild steatosis was present focally, with a small number of apoptotic hepatocytes. Moderate to severe inflammatory cellular infiltration appeared on day 6, with more extensive steatosis, and severe necrapoptosis. On day 8, there was only residual steatosis, accompanied by markedly reduced inflammation. Numerous mitotic figures observed at this time indicated early hepatocellular regeneration. By day 12 after infection, most of hepatocytes appeared normal. YFV-specific antigen was detected in

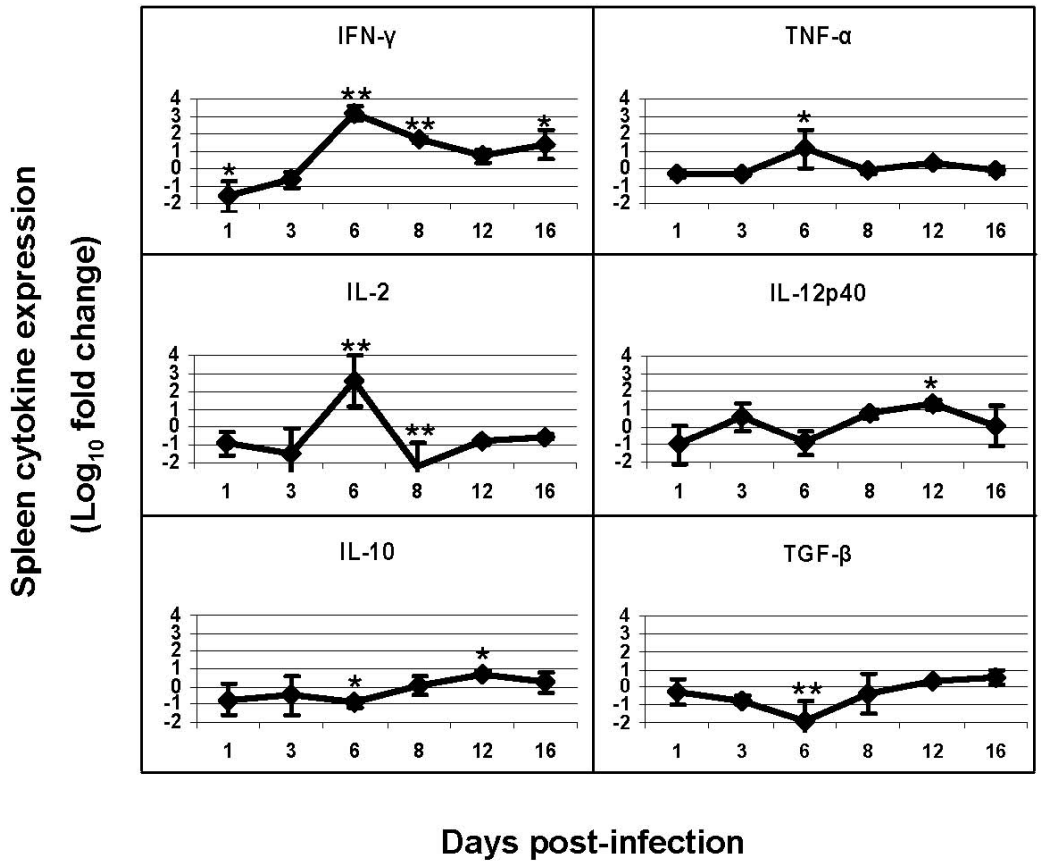

Figure 4 Expression of inflammatory and regulatory cytokines in the spleens of YFV-infected hamsters. Mean $\log_{10}$ fold change (± SD) are shown for 4 animals per data point. Fold changes vs control were determined by $2^{-\Delta\Delta Ct}$, where $\Delta\Delta C_t = \Delta C_{t\ (infected)} - \Delta C_{t\ (uninfected)}$ and $\Delta C_t = C_{t\ (target\ gene)} - C_{t\ (ß\text{-}actin\ gene)}$. * and ** indicate $p<0.05$ and $p<0.01$, respectively, between infected and uninfected animals.

sections of the liver with the strongest appearance occurring from days 3 to 8.

The mRNA levels of Th1-type inflammatory cytokines (IFN-γ, IL-2, IL-12p40, and TNF-α) and Th2-type regulatory cytokines (IL-4, IL-10 and TGF-ß) at different time points of infection were measured and compared to those of uninfected controls. As shown in **Figure 3**, when compared to uninfected animals, the inflammatory cytokines were slightly elevated on day 3, decreased on days 6 and 8 and then, elevated again on day 12.

As for the regulatory cytokines, IL-10 was elevated on day 6 by 52-fold ($p<0.01$), and on day 12 by 85-fold ($p<0.01$). TGF-β was decreased on day 6 and 8, and elevated on day 12 by 3-fold. Expression of IL-4 was undetectable.

Pathology and Cytokine Responses in the Spleen

The microscopic abnormalities in the spleen included reactive lymphoid hyperplasia initially, characterized by expansion of the white pulp, and followed by marked depletion of lymphocytes. YFV-antigens were detected by IHC on days 6 and 8. For inflammatory cytokines, the expression patterns in spleen were almost opposite to that in the liver, with peak elevations occurring on days 6 and 8 (**Figure 4**). On day 6, IFN-γ was significantly elevated by 1478-fold ($p< 0.005$), IL-2 by 364-fold ($p<0.005$), and TNF-α by 12-fold ($p<0.05$). The regulatory cytokines showed little change at early and mid-stages of infection, but were elevated at late-stage. On day 12, IL-10 increased by 5-fold ($p<0.05$) and TGF-β increased by 2-fold. IL-4 expression was sporadic and insignificant.

Pathology and Cytokine Responses in the Kidney

Histologic changes in the kidneys included degeneration of tubular epithelium, with diffuse swelling and collapse of the tubular lumen. The affected tubular epithelial cells exhibited dense eosinophilic cytoplasm and condensed nuclei (features of early acute tubular necrosis). Inflammatory cytokines in the kidneys were significantly increased (**Figure 5**), peaking on day 6 of infection. IFN-γ was increased by 17-fold, IL-2 was increased by 5-fold, and TNF-α was increased by 10-fold ($p<0.01$). IL-12p40 was increased during mid- and late-stages. Among the regulatory cytokines, IL-10 was significantly elevated throughout the course of infection. To a lesser degree, TGF-β was also elevated on days 6 and 12. IL-4 expression was insignificant at all tested time points.

Pathology and Cytokine Responses in the Heart

In general, no specific morphologic abnormalities were identified in the myocardial tissue. YFV-specific antigens were identified in this organ only on day 8. **Figure 6** shows that most inflammatory cytokines were significantly increased after infection, peaking on day 6, with IFN-γ significantly increased by 152-fold ($p<0.005$), IL-2 by 906-fold ($p<0.001$), and TNF-α by 11-fold ($p<0.05$). The pattern of regulatory cytokine expression in the heart was similar to that of the kidneys. IL-10 was maintained at high levels during the infection, while TGF-β was slightly decreased. IL-4 expression was insignificant at all tested time points.

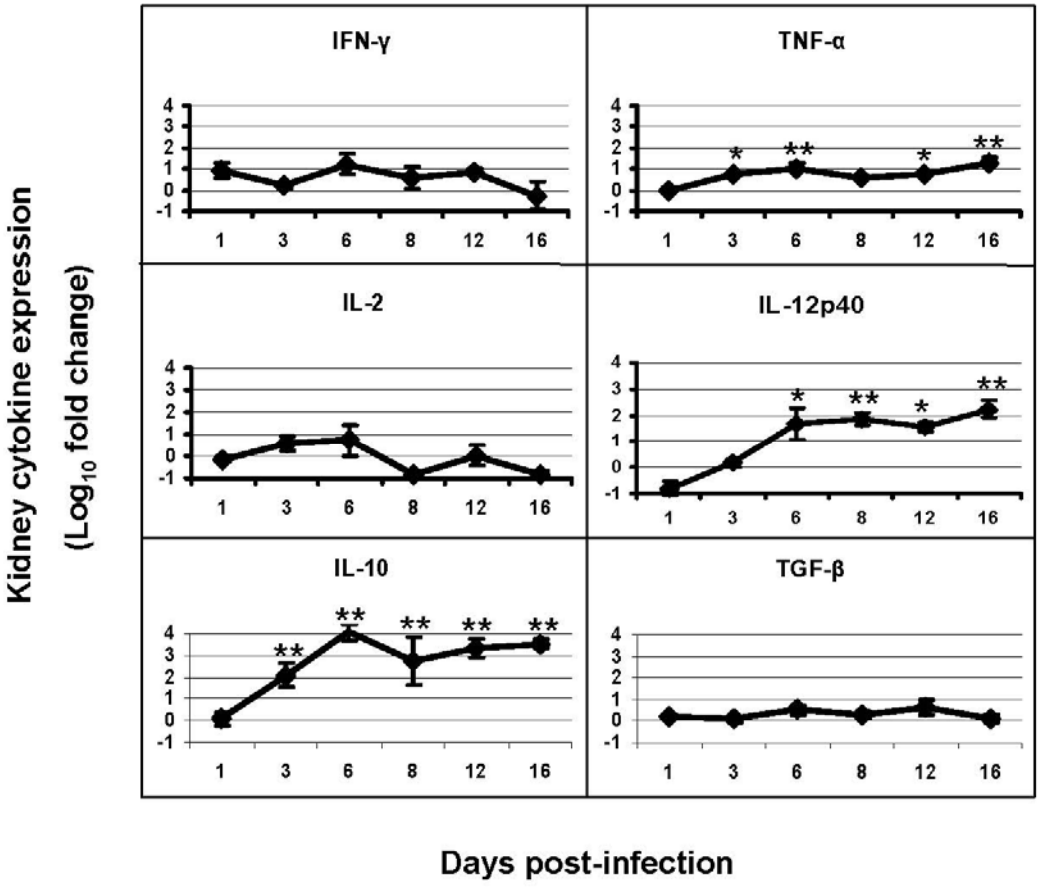

Figure 5 Expression of inflammatory and regulatory cytokines in the kidneys of YFV-infected hamsters. Mean $\log_{10}$ fold change (± SD) are shown for 4 animals per data point. Fold changes vs. control were determined by $2^{-\Delta\Delta Ct}$, where $\Delta\Delta C_t = \Delta C_{t\ (infected)} - \Delta C_{t\ (uninfected)}$ and $\Delta C_t = C_{t\ (target\ gene)} - C_{t\ (ß\text{-}actin\ gene)}$. * and ** indicate $p<0.05$ and $p<0.01$, respectively, between infected and uninfected animals.

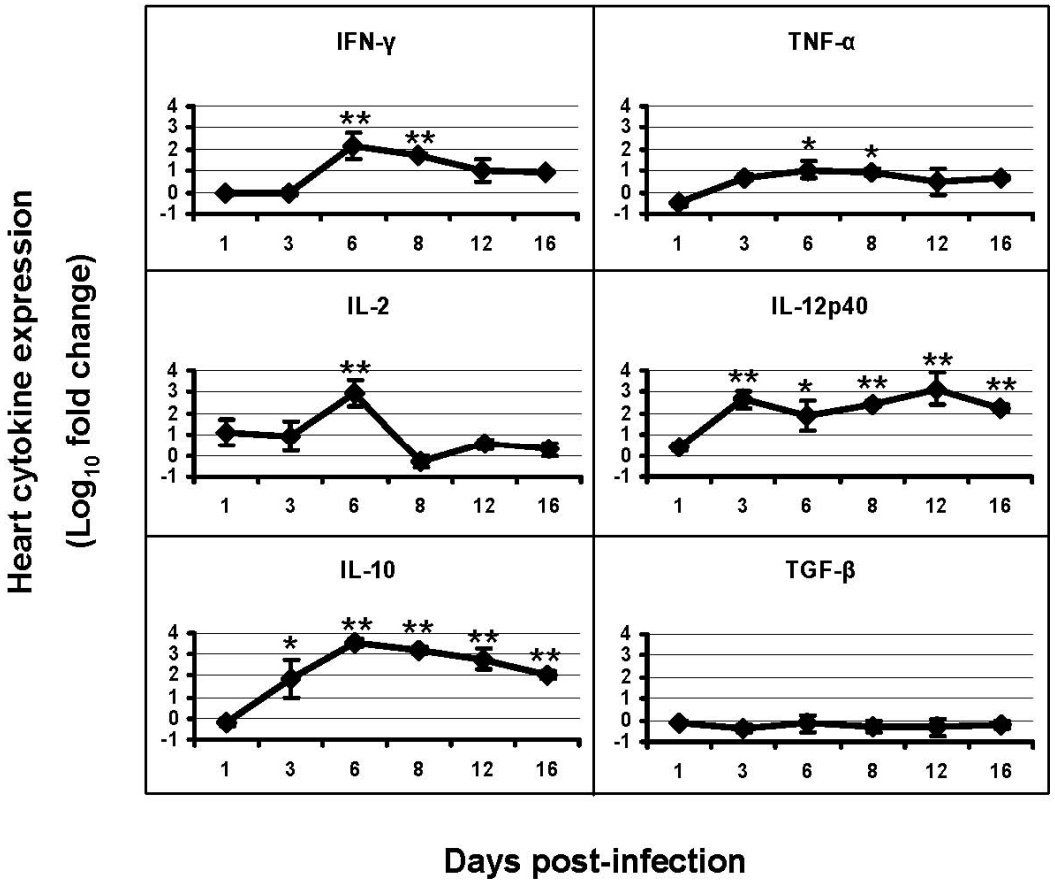

Figure 6 Expression of inflammatory and regulatory cytokines in the hearts of YFV-infected hamsters. Mean log_{10} fold change (± SD) are shown for 4 animals per data point. Fold changes vs. control were determined by $2^{-\Delta\Delta Ct}$, where $\Delta\Delta C_t = \Delta C_{t\ (infected)} - \Delta C_{t\ (uninfected)}$ and $\Delta C_t = C_{t\ (target\ gene)} - C_{t\ (ß\text{-}actin\ gene)}$. * and ** indicate $p<0.05$ and $p<0.01$, respectively, between infected and uninfected animals.

Discussion

Previously published studies on yellow fever pathogenesis have mostly focused on the clinical manifestations and histological alterations in YFV infections [1, 21, 22], with limited description on the mechanisms of cell injury, or type of local immune responses. Knowledge of these mechanisms is important in developing better treatments for this disease. Studies of experimentally-induced disease in non-human primates and hamsters [10, 11] have shown that lymphoid tissues are one of the major targets of YFV. The depletion of lymphoid tissues seen in YFV-infected hamsters [11] is very similar to that of Ebola infection [23]. Rhesus and vervet monkeys infected intraperitoneally with Ebola virus develop an acute hemorrhagic fever with acute necrosis in the liver, spleen, lymph nodes, and lungs [24], with abnormal cytokine expression profiles [25, 26]. In our hamster model of YF, the animals die between the sixth and tenth day after infection, when the level of viremia is low or undetectable in blood [10], suggesting that death of animals may be correlated to host immune responses. We postulated that tissue injuries caused by YFV infection are due to a combination of factors, namely direct viral injury and harmful immune responses by the host.

Antiviral defense mechanisms in vertebrates are numerous, ranging from relatively primitive, constitutively expressed and non-specific defenses to sophisticated mechanisms that are specifically induced in response to the invading virus. Natural killer cells and type 1 IFNs protect the host during the early phase of virus replication, before the

appearance of specific CTL and antibodies [27]. Cytokines, produced largely by macrophages and T lymphocytes, also play a pivotal role in antiviral immune responses [28, 29].

Due to the lack of immunological reagents to study hamster cytokine responses, Northern blot had been used as an alternative to examine cytokine expression in a hamster model of visceral leishmaniasis [30]; however, this assay requires a large amount of total RNA (30 μg), and it is difficult to accurately quantify differences among multiple samples. Therefore, in this study, we used real-time quantitative RT-PCR to examine cytokine expression profiles in the liver, spleen, heart, and kidneys during YFV infection. The latter assay requires small amounts (1 μg) of total RNA, and allows accurate comparisons between large numbers of samples.

We found that as early as day 3 of infection, there was evident increase in Th1 cytokines in some organs, suggesting that their response might be the host's attempt to control the viral infection. In the mid-stage of infection when hepatic damage was distinct and viral antigens were abundant, there was marked reduction of Th1 cytokines in the liver. The cause of this reduction is unclear, and further studies are needed to determine whether this was caused by the passive clearance of the initial inflammatory cytokine response to virus, virus suppression of the cytokine response, regulatory cytokines, or by a combination of these mechanisms. Interestingly, the pattern of inflammatory cytokines in the spleen, kidneys, and heart was contrary to that of the liver at the mid-stage of infection (day 6). The elevated expression of Th1 cytokines in these organs suggests a protective role of these cytokines against YFV infection, since they are important effectors in cell-mediated responses to virus infection [27-29, 31]. IFN-γ plays a key role in the control of infection with many intracellular pathogens and is the primary cytokine responsible for macrophage activation and killing of virus. IL-12 is a heterodimeric cytokine, strongly promoting the differentiation of naïve $CD4^+$ T cells to the Th1 phenotype and suppressing the expression of Th2 cytokines [32]. It is also a strong inducer of IFN-γ production. TNF-α has both protective and pathologic consequences for the host, and can act synergistically with IFN-γ to activate macrophages to kill virus and promote resolution of virus infection [33].

Another important observation in this study was that all of the tested cytokines were elevated in the late-stage of infection. There were also abnormalities in the liver function studies and organ pathology on day 16. The levels of ALT and AST were elevated, suggesting an immunopathogenic mechanism related to progression of disease in the absence of virus replication. Inflammatory cytokines may have contributed to this immunopathology. IFN-γ is a potent inducer of nitric oxide (NO) production by macrophages. NO can exert pathogenic effects by suppressing T cell responses [34]. TNF-α also has been reported to contribute to cell death in certain situations [14]. In humans, hypotension and shock occur in the late-stage of YFV infection and are probably mediated by cytokine dysregulation. IFN-γ, TNF-α, and other cytokines produced by activated Kupffer cells and splenic macrophages in response to direct YFV injury and CTLs involved in viral clearance might also be responsible for cell injury, oxygen-free radical formation, endothelial damage and microthrombosis, disseminated intravascular coagulation, tissue anoxia, oliguria, and shock.

IL-10 has been demonstrated to antagonize Th1 cytokine synthesis and to inhibit macrophage activation and killing of intracellular pathogens. After YFV infection, we found increased IL-10 expression in the hamster spleen over time, suggesting a role for IL-10 in disease progression and suppression of T cell function. TGF-β has been shown to exacerbate virus infection in monkeys and humans [35, 36]; we also observed that the expression of TGF-β mRNA increased during late-stages of infection in the liver, spleen and kidneys. Their increase may be associated with tissues damage.

The expression of IL-4 was very low in both healthy and YFV-infected hamster tissues. This is in striking contrast to observations made in mice, in which IL-4 has been shown to be important in infection with certain intracellular pathogens [36]. For some pathogens, such as *Leishmania major*, IL-4 has a deleterious effect on the outcome of infection and appears to down-regulate or prevent the induction of protective immune responses [37, 38].

In summary, we report the first detailed study of cytokine responses during experimental YFV infection and their relationship to organ pathology in a hamster model of YF. Results of our study suggest that immune responses to YFV in the liver is compromised at the mid-stages of infection, possibly due to direct viral injury to the hepatic cells and lymphoid tissues, and that the immunopathogenic mechanism is related to progression of disease in the late-stage of infection.

Acknowledgements

The authors wish to thank Judith Aronson, John Pfeifer and Shang Lei for their advice in statistical and data analyses. This work was supported by grants from the National Institute of Health (NIH) AI 25489 and AI056196.

Please address all correspondences to Shu-Yuan Xiao, MD, Department of Pathology, University of Texas Medical Branch, 301 University Boulevard, Galveston, TX 77555-0588, USA. Tel: 409-772-8447; Fax: 409-747-2429; Email: syxiao@utmb.edu

References

[1] Robertson SE, Hull BP, Tomori O, Bele O, LeDuc JW and Esteves K. Yellow fever: A decade of reemergence. *JAMA* 1996;276:1157-1162.

[2] Monath TP. Yellow fever: a medically neglected disease: report on a seminar. *Rev Infect Dis* 1987;9:165-175.

[3] Monath TP and Barrett AD. Pathogenesis and pathophysiology of yellow fever. *Adv Virus Res* 2003;60:343-95.

[4].Monath TP. Yellow fever. In Monath TP (ed): The arboviruses: epidemiology and ecology. CRC Press, Boca Raton, FL. 1989; Vol 5, pp139-231.

[5] Monath TP. Yellow fever: an update. *The Lancet Infectious Diseases*. 2001;1:1120.

[6] Monath TP. Yellow fever. In Guerrant RL, Walker DH and Weller PF (Eds): Tropical infectious diseases. Vol 2. Churchill Livingstone, Philadelphia. 1999, pp1253-1264.

[7] Hudson NP. The pathology of experimental yellow fever in the Macacus rhesus. III. Comparison with the pathology of yellow fever in man. *Am J Pathol* 1928;4:41939.

[8] Bugher JC. The pathology of yellow fever. In Strode GK (Ed) Yellow fever. McGraw-Hill, New York City. 1951, pp137-163.

[9] Del Rio C and Meier FA. Yellow fever. In Nelson AM and Horsburgh CR Jr (Eds): Pathology of emerging infection 2. American Society for Microbiology, Washington DC. 1998, pp13-41.

[10] Tesh RB, Guzman H, da Rosa AP, Vasconcelos PF, Dias LB, Bunnell JE, Zhang H and Xiao SY. Experimental yellow fever virus infection in the Golden Hamster (Mesocricetus auratus). I. Virologic, biochemical, and immunologic studies. *J Infect Dis* 2001;183:1431-1436.

[11] Xiao SY, Zhang H, Guzman H and Tesh RB. Experimental yellow fever virus infection in the Golden hamster (Mesocricetus auratus). II. Pathology. *J Infect Dis* 2001;183:1437-1444.

[12] Liu T and Chambers T J. Yellow fever virus encephalitis: properties of the brain-associated T-cell response during virus clearance in normal and Gamma interferon-deficient mice and requirement for CD4+ lymphocytes. *J Virol* 2001;75:2107-2118.

[13] Wodarz D, Christensen JP and Thomsen AR. The importance of lytic and nonlytic immune responses in viral infections. *Trends Immunol* 2002;23:194-200.

[14] Seewaldt S, Thomas HE, Ejrnaes M, Christen U, Wolfe T, Rodrigo E, Coon B, Michelsen B, Kay TW and von Herrath MG. Virus-induced autoimmune diabetes: most beta-cells die through inflammatory cytokines and not perforin from autoreactive (anti-viral) cytotoxic T-lymphocytes. *Diabetes* 2000;49:1801-9.

[15] Sbrana E, Xiao SY, Guzman H, Ye M, Travassos da Rosa AP and Tesh RB. Efficacy of post-exposure treatment of yellow fever with ribavirin in a hamster model of the disease. *Am J Trop Med Hyg* 2004;71:306-312.

[16] Reed LJ and Muench H. A single method of estimating fifty percent end points. *Am J Hyg* 1938;27:493-497.

[17] Livak KJ and Schmittgen TD. Analysis of relative gene expression data using real-time quantitative PCR and the $2^{-\Delta\Delta Ct}$ method. *Methods* 2001;25:402-408.

[18] Kipar A, Leutenegger CM, Hetzel U, Akens MK, Mislin CN, Reinacher M and Lutz H. Cytokine mRNA levels in isolated feline monocytes. *Vet Immunol Immunopath* 2001;78:305-315.

[19] Tomori O. Yellow fever: the recurring plague. *Crit Rev Clin Lab Sci* 2004;41: 391-427.

[20] Barrett AD and Monath TP. Epidemiology and ecology of yellow fever virus. *Adv Virus Res* 2003; 61:291-315.

[21] Vasconcelos PFC, Bryant JE, Travassos da Rosa APA, Tesh RB, Rodrigues SG and Barrett ADT. Genetic divergence and dispersal of yellow fever virus. *Brazil Emerg Infect Dis* 2004;10: 1578–1584.

[22] Vasconcelos PFC, Travassos da Rosa APA, Rodrigues SG, Rosa EST, Monteiro HAO, Cruz ACR, Barros VLRS, Souza MR and Rosa JFST. Yellow fever in Para State, Amazon region of Brazil, 1998–1999: entomologic and epidemiologic findings. *Emerg Infect Dis* 2001; 7: 565-569.

[23] Ikegami T, Miranda ME, Calaor AB, Manalo DL, Miranda NJ, Niikura M, Saijo M, Une Y, Nomura Y, Kurane I, Ksiazek TG, Yoshikawa Y and Morikawa S. Histopathology of natural Ebola

virus subtype Reston infection in cynomolgus macaques during the Philippine outbreak in 1996. *Exp Anim* 2002;51: 447-455.

[24] Baskerville A, Bowen ET, Platt GS, McArdell LB and Simpson DI. The pathology of experimental Ebola virus infection in monkeys. *J Pathol* 1978;125: 131-138.

[25] Leroy EM, Baize S, Debre P, Lansoud SJ and Mavoungou E. Early immune responses accompanying human asymptomatic Ebola infections. *Clin Exp Immunol* 2001;124:453-460.

[26] Hutchinson KL, Villinger F, Miranda ME, Ksiazek TG, Peters CJ and Rollin PE. Multiplex analysis of cytokines in the blood of cynomolgus macaques naturally infected with Ebola virus (Reston serotype). *J Med Virol* 2001;65: 561-566.

[27] Czarniecki CW, Fennie CW, Powers DB and Estell DA. Synergistic antiviral and antiproliferative activities of Escherichia coli-derived human alpha, beta, and gamma interferons. *J Virol* 1984;49:490-496.

[28] Grace HWW and David VG. Tumour necrosis factors alpha and beta inhibit virus replication and synergize with interferons. *Nature* 1986; 323:819-822.

[29] Karp BI, Yang JC, Khorsand M, Wood R and Merigan TC. Multiple cerebral lesions complicating therapy with interleukin-2. *Neurology* 1996;47:417-424.

[30] Melby PC, Tryon VV, Chandrasekar B and Freeman GL. Cloning of Syrian hamster (Mesocricetus auratus) cytokine cDNAs and analysis of cytokine mRNA expression in experimental visceral leishmaniasis. *Infect Immun* 1998;66:2135-2142.

[31] Estes DM, Hirano A, Heussler VT, Dobbelaere DA and Brown WC. Expression and biological activities of bovine interleukin 4: effects of recombinant bovine interleukin 4 on T cell proliferation and B cell differentiation and proliferation in vitro. *Cell Immunol* 1995; 163:268-279.

[32] Trinchieri G. Interleukin-12: a proinflammatory cytokine with immunoregulatory functions that bridge innate resistance and antigen-specific adaptive immunity. *Annu Rev Immunol* 1995; 13: 251-276.

[33] Asper M, Sternsdorf T, Hass M, Drosten C, Rhode A, Schmitz H and Günther S. Inhibition of different Lassa virus strains by alpha and gamma interferons and comparison with a less pathogenic arenavirus. *J Virol* 2004;78:3162-3169.

[34] Akaike T. Role of free radicals in viral pathogenesis and mutation. *Rev Med Virol* 2001;11:87-101.

[35] Quaresma JAS, Barros VLRS, Pagliari C, Fernandes ER, Guedes F, Takakura CFH, Andrade, Jr HF, Vasconcelos PFC and Duarte MIS. Revisiting the liver in human yellow fever: Virus-induced apoptosis in hepatocytes associated with TGF-β, TNF-α and NK cells activity. *Virology* 2006;345:22-30.

[36] Newton C, McHugn S, Widen R, Nakachi N, Klein T and Friedman H. Induction of Interleukin-4 (IL-4) by Legionella pneumophila infection in BALB/c mice and regulation of tumor necrosis factor alpha, IL-6, and IL-1β. *Infect Immun* 2000;68:5234-5240.

[37] Chatelain R, Varkila K and Coffman RL. IL-4 induces a Th2 response in Leishmania major-infected mice. *J Immunol* 1992;148:1182–1187.

[38] Nabors GS and Farrell JP. Depletion of interleukin-4 in BALB/c mice with established *Leishmania major* infections increases the efficacy of antimony therapy and promotes Th1-like responses. *Infect Immun* 1994; 62:5498-5504.